Science Advances
AAAS

Supplementary Materials for

The risk variant rs11836367 contributes to breast cancer onset and metastasis by attenuating Wnt signaling via regulating NTN4 expression

Han Yang *et al.*

Corresponding author: Xin-Xia Tian, tianxinxia@bjmu.edu.cn

Sci. Adv. **8**, eabn3509 (2022)
DOI: 10.1126/sciadv.abn3509

The PDF file includes:

Other Supplementary Material for this manuscript includes the following:

Fig. S1.

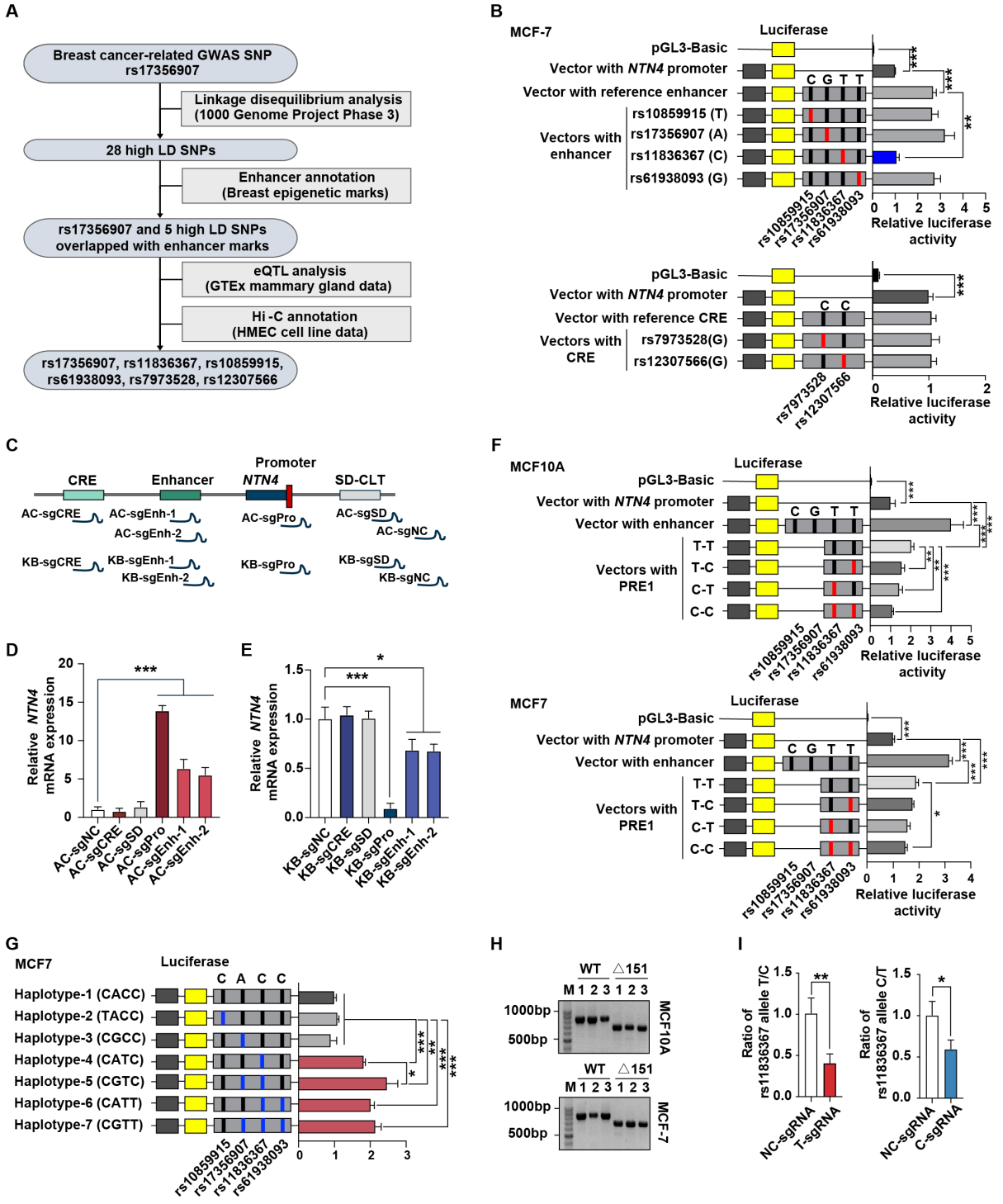

Fig. S1. rs11836367 regulates *NTN4* expression. Related to Fig. 1.

(A) Flowchart of studying GWAS breast cancer susceptible SNP rs17356907 in enhancer region. **(B)** Luciferase reporter assays after transient transfection of MCF-7 breast cancer cells with different constructs. DNA fragments containing different alleles of the GWAS-SNP rs17356907 and its LD-SNPs in enhancer or cis-regulatory element (CRE) were cloned into *NTN4*-promoter-

driven luciferase constructs. Luciferase signals were normalized to renilla signals. **(C)** Schematic illustrating the sgRNAs designed to target different loci in CRISPR-activation (CRISPRa) and CRISPR-interference (CRISPRi) assays. AC-sgNC and KB-sgNC contain non-targeting control guide RNA. Negative control AC-sgSD and KB-sgSD contain a guide RNA targeting a locus, which is the same distance from the *NTN4* promoter as enhancer. Positive control AC-sgPro and KB-sgPro target the *NTN4* promoter. AC-sgEnh-1, AC-sgEnh-2, KB-sgEnh-1 and KB-sgEnh-2 target enhancer. AC-sgCRE and KB-sgCRE target CRE. **(D** and **E)** sgRNAs illustrated in (C) were used for CRISPRa in MCF-7 cells (D) or for CRISPRi in MCF10A cells (E), and *NTN4* mRNA expression was measured by qRT-PCR. **(F)** Luciferase reporter assays after transient transfection of MCF10A and MCF-7 cells with different constructs. DNA fragments containing different alleles of the GWAS-SNP rs17356907 and its LD-SNPs in enhancer and PRE1 were cloned into *NTN4*-promoter-driven luciferase constructs. Luciferase signals were normalized to renilla signals. **(G)** The luciferase reporter assay was performed after transient transfection of MCF-7 cells with *NTN4*-promoter-driven luciferase vectors containing different haplotypes of 4 SNPs (rs10859915, rs17356907, rs11836367 and rs61938093). Luciferase signals were normalized to renilla signals. **(H)** Gel image showing PCR amplification of the rs11836367 region in wild type (WT) and 151 bp deletion clones (▵151) in MCF10A and MCF7 cell lines. M: DNA Marker. **(I)** Bar plot showing allele-specific T-sgRNA and C-sgRNA preferentially introduced the T and C alleles of rs11836367 respectively when coupled with Cas9-NG. Data are represented as mean ± SEM. *$P \leq 0.05$, **$P \leq 0.01$, ***$P \leq 0.001$. *P* values in (B, D, E, F and G) were determined by two-way ANOVA followed by Dunnett's multiple comparisons test. *P* values in (I) were determined Student's t-test. Data are representative of three independent experiments.

Fig. S2.

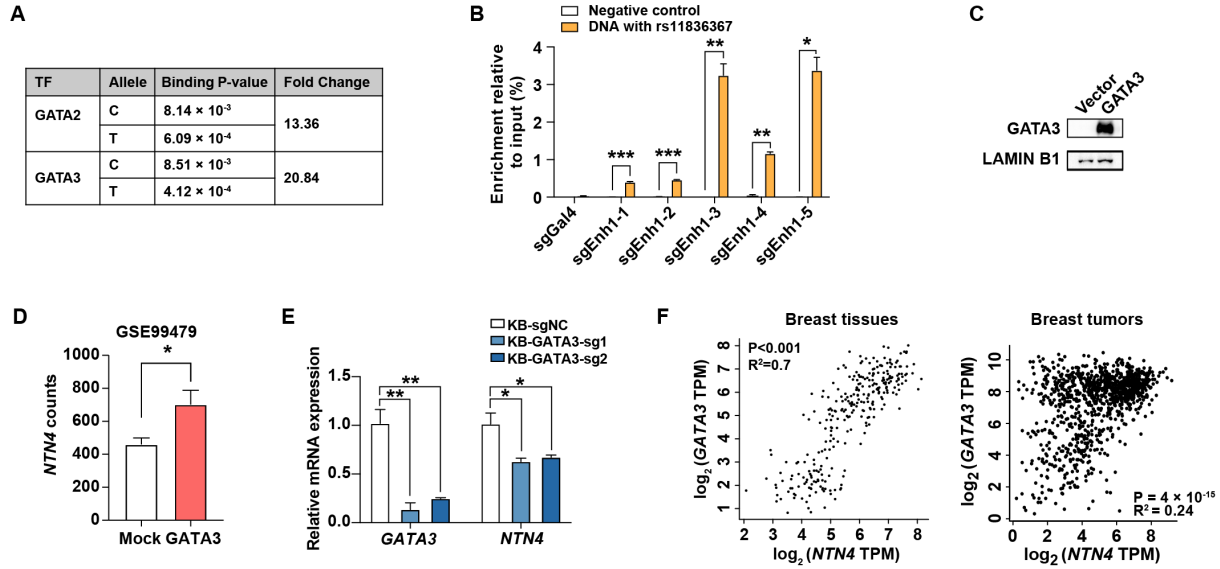

TF	Allele	Binding P-value	Fold Change
GATA2	C	8.14×10^{-3}	13.36
	T	6.09×10^{-4}	
GATA3	C	8.51×10^{-3}	20.84
	T	4.12×10^{-4}	

Fig. S2. rs11836367 allele specifically influences GATA3 binding affinity. Related to Fig. 2.

(A) Predicted binding affinity of GATA2 and GATA3 with different allele of rs11836367 through PERFECTPS-APE software. **(B)** ChIP-qPCR confirmed the capture-efficiency of several sgRNAs used for *in-situ* Capture assay. sgEnh1-1/2/3/4/5 target enhancer containing rs11836367, and non-targeting sgGal4 is a negative control. sgEnh1-3 and sgEnh1-5 have higher capture efficiency for DNA containing the rs11836367 locus. **(C)** Overexpression of GATA3 in 293T nuclear extracts validated by western blotting. (**D)** RNA-seq of T47D (GSE99479) showed that overexpression of GATA3 in T-47D increased *NTN4* expression. **(E)** qRT-PCR analysis of the *GATA3* and *NTN4* expression in the control or *GATA3* knockdown cells line MCF7-dCas9-KRAB by CRISPRi. **(F)** The correlation analysis of *NTN4* expression with *GATA3* expression in normal breast tissues and breast cancer tissues from TCGA using GEPIA. Data are represented as mean ± SEM. **P* ≤ 0.05, ***P* ≤ 0.01, ****P* ≤ 0.001. *P* value in figures (B, D and E) were calculated using the Student's t-test. Data in figures (B and E) are representative of two to three independent experiments.

Fig. S3.

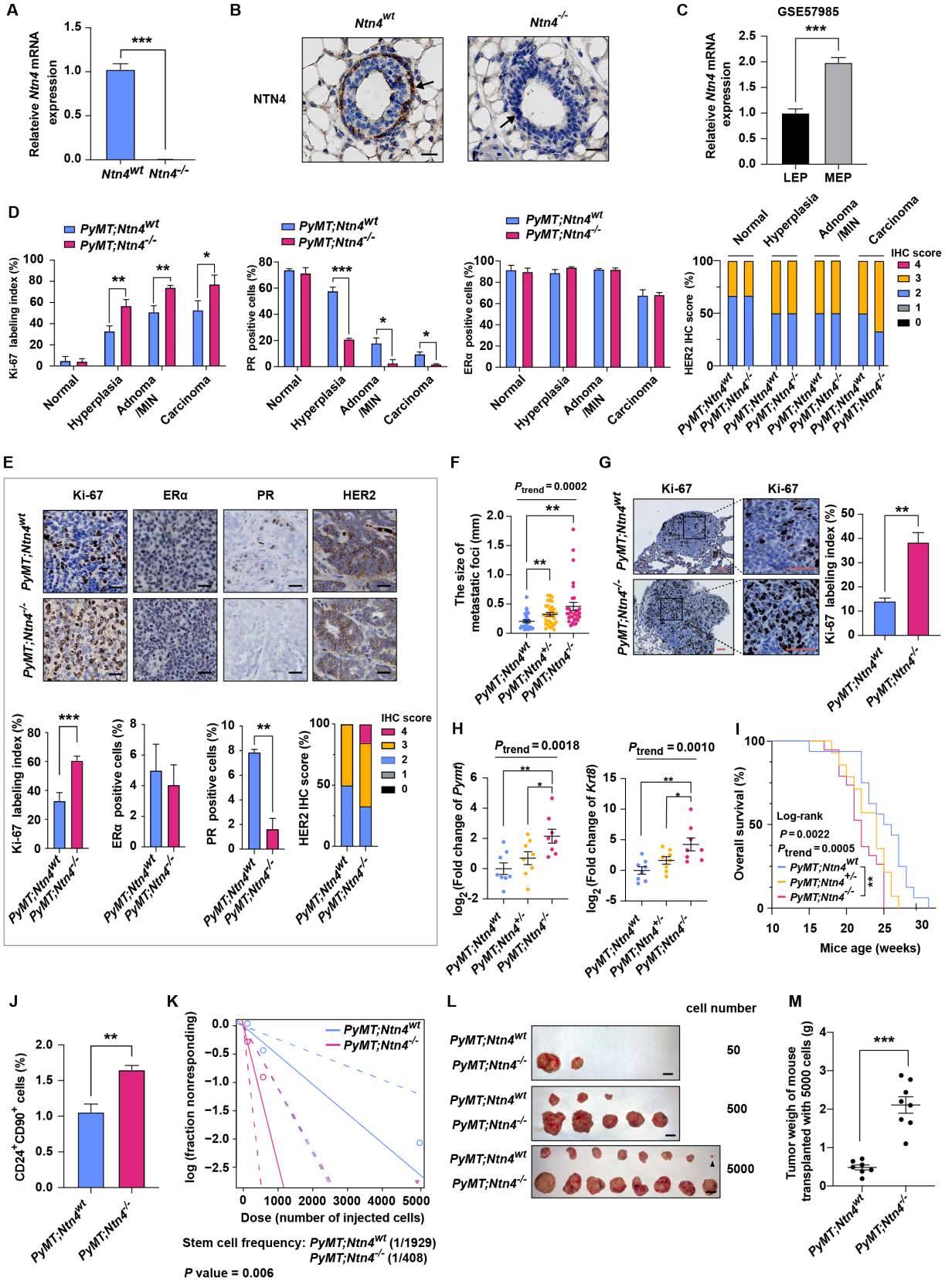
A
Relateive Ntn4 mRNA expression
Ntn4wt Ntn4-/-
B
Ntn4wt
Ntn4-/-
NTN4
C
GSE57985
Relateive Ntn4 mRNA expression
LEP
MEP
D
PyMT;Ntn4wt
PyMT;Ntn4-/-
Ki-67 labeling index (%)
PR positive cells (%)
ERα positive cells (%)
HER2 IHC score (%)
IHC score
Normal
Hyperplasia
Adnoma /MIN
Carcinoma
E
Ki-67
ERα
PR
HER2
F
Ptrend = 0.0002
The size of metastatic foci (mm)
PyMT;Ntn4wt
PyMT;Ntn4+/-
PyMT;Ntn4-/-
G
Ki-67
Ki-67 labeling index (%)
H
Ptrend = 0.0018
Ptrend = 0.0010
log2(Fold change of Pymt)
log2(Fold change of Krt8)
I
Log-rank
P = 0.0022
Ptrend = 0.0005
Overall survival (%)
Mice age (weeks)
J
CD24+CD90+ cells (%)
K
log (fraction nonresponding)
Dose (number of injected cells)
Stem cell frequency: PyMT;Ntn4wt (1/1929)
PyMT;Ntn4-/- (1/408)
P value = 0.006
L
cell number
50
500
5000
M
Tumor weigh of mouse transplanted with 5000 cells (g)

Fig. S3. Loss of *Ntn4* in *PyMT* mice affected mammary tumor progression, metastasis and cancer stem cells. Related to Fig. 3.

(A and B) Expressions of *Ntn4* mRNA and NTN4 protein in the mammary gland were examined by qRT-PCR (A) and Immunohistochemical staining (B) respectively. n = 3 for both groups. As indicated by the arrow, *Ntn4* is mainly expressed by myoepithelial cells in wild-type (WT) mammary glands, but is absent in $Ntn4^{-/-}$ mice. Scale bar, 20 μm. **(C)** The expression of *Ntn4* is higher in myoepithelial cells (MEP) than in luminal epithelial cells (LEP) based on microarray data GSE7513. **(D)** Quantification of Ki-67, ER, PR and HER2 in different stages of tumors of 13-week-old $PyMT;Ntn4^{wt}$ and $PyMT;Ntn4^{-/-}$ mice. n = 3-6 for both groups. **(E)** Representative images of IHC staining (upper) and quantification (lower) of Ki-67, ER, PR and HER2 in the late-stage tumors of $PyMT;Ntn4^{wt}$ and $PyMT;Ntn4^{-/-}$ mice. n = 3-6 for both groups. Scale bar, 20 μm. **(F)** The size of metastatic foci in the lung sections was measured in $PyMT;Ntn4^{wt}$, $PyMT;Ntn4^{+/-}$ and $PyMT;Ntn4^{-/-}$ at the endpoint. n > 25 for each group. **(G)** Representative images of IHC staining for Ki-67 (left) and quantification of Ki-67 labeling index (right) in the lung sections of $PyMT;Ntn4^{wt}$ and $PyMT;Ntn4^{-/-}$ late-stage mice. n = 3 for both groups. Scale bar, 50 μm. **(H)** qRT-PCR examination of *Pymt and Krt8* expression in blood samples was used as a measure of circulating cancer cells in $PyMT;Ntn4^{wt}$, $PyMT;Ntn4^{+/-}$ and $PyMT;Ntn4^{-/-}$ mice. n = 8 for each group. **(I)** Kaplan-Meier analysis of overall survival in $PyMT;Ntn4^{wt}$ (n = 16), $PyMT;Ntn4^{+/-}$ (n = 14) and $PyMT;Ntn4^{-/-}$ (n = 18) mice. Mice were euthanized when the largest tumor reached 2 cm in diameter. **(J)** $CD24^{+}CD90^{+}$ cells in $PyMT;Ntn4^{wt}$ (n=3) and $PyMT;Ntn4^{-/-}$ tumors (n=3) were quantified by flow cytometry. **(K)** Limiting dilution assay demonstrated the tumor-initiating frequencies of primary tumor cells isolated from $PyMT;Ntn4^{wt}$ and $PyMT;Ntn4^{-/-}$ mice. **(L)** Pictures of tumors in three groups transplanted with 50, 500, 5000 of $PyMT;Ntn4^{wt}$ and $PyMT;Ntn4^{-/-}$ tumor cells. Mice transplanted with 5000 cells were sacrificed after 4 weeks of transplantation, and the mice transplanted with 50 and 500 cells were sacrificed after 8 weeks of transplantation. Arrowheads point to fat pads (no tumors). Scale bar, 1 cm. **(M)** Tumor weight transplanted with 5000 tumor cells of $PyMT;Ntn4^{wt}$ and $PyMT;Ntn4^{-/-}$ after 4 weeks of transplantation. Data are represented as mean ± SEM. $*P \leq 0.05$, $**P \leq 0.01$, $***P \leq 0.001$. *P* values in figure (A, C, D, E, G, J and M) were calculated using Student's t-test. P_{trend} values in figures (F and H) were determined by one-way ANOVA and *P* values between two groups were determined by one-way ANOVA followed by Dunnett's multiple comparisons test. Data in figure (I) was first calculated by comparing three groups for log-rank *P* value and P_{trend} value, and *P* values between two groups were further calculated using log-rank test adjusted with Bonferroni correction.

Fig. S4.

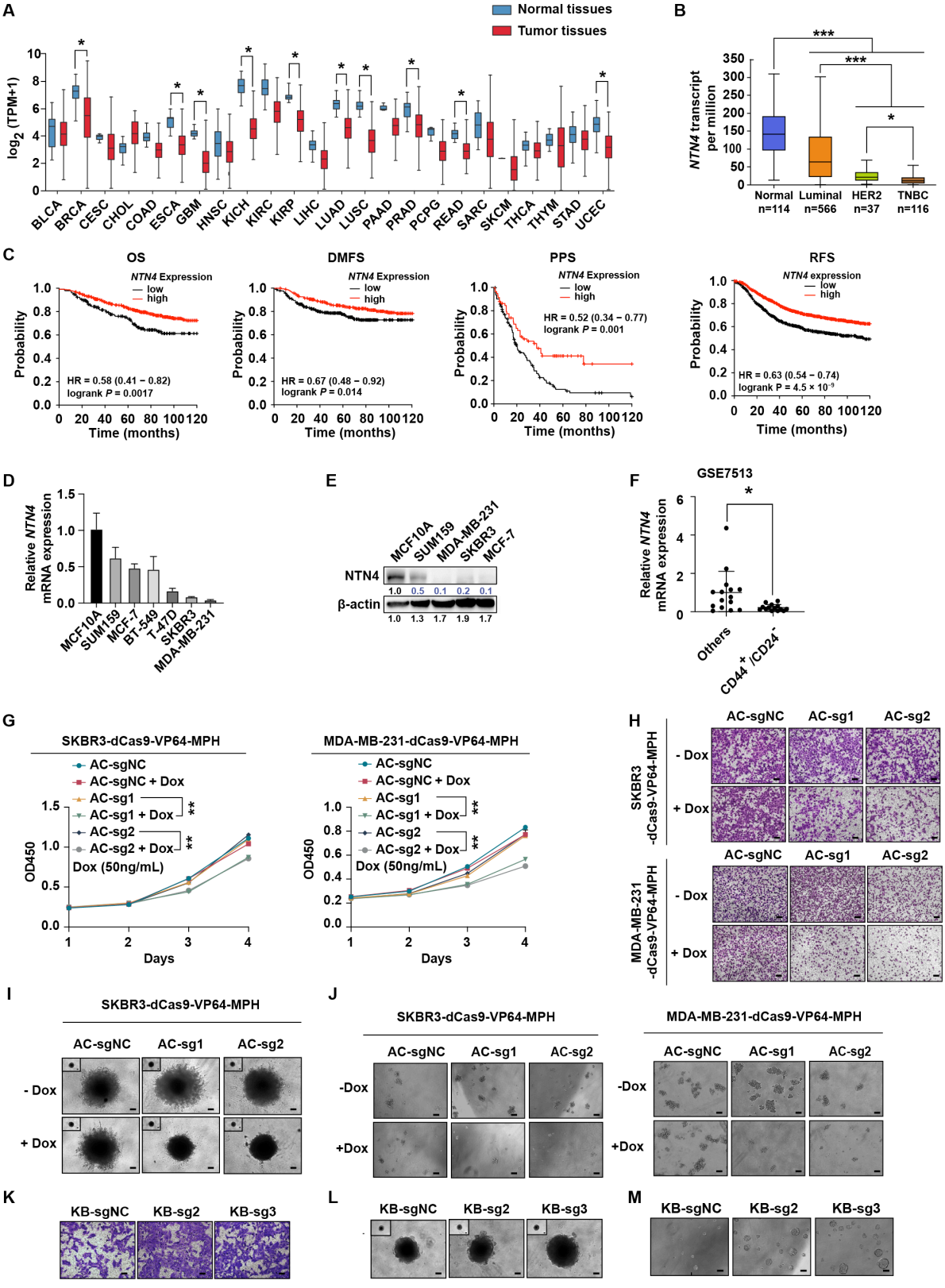
A
Normal tissues
Tumor tissues
log2 (TPM+1)
BLCA BRCA CESC CHOL COAD ESCA GBM HNSC KICH KIRC KIRP LIHC LUAD LUSC PAAD PRAD PCPG READ SARC SKCM THCA THYM STAD UCEC
B
NTN4 transcript per million
Normal n=114
Luminal n=566
HER2 n=37
TNBC n=116
C
OS
DMFS
PPS
RFS
NTN4 Expression
low
high
Probability
Time (months)
HR = 0.58 (0.41 − 0.82)
logrank P = 0.0017
HR = 0.67 (0.48 − 0.92)
logrank P = 0.014
HR = 0.52 (0.34 − 0.77)
logrank P = 0.001
HR = 0.63 (0.54 − 0.74)
logrank P = 4.5 × 10-9
D
Relative NTN4 mRNA expression
MCF10A SUM159 MCF-7 BT-549 T-47D SKBR3 MDA-MB-231
E
MCF10A SUM159 MDA-MB-231 SKBR3 MCF-7
NTN4
β-actin
1.0 0.5 0.1 0.2 0.1
1.0 1.3 1.7 1.9 1.7
F
GSE7513
Relative NTN4 mRNA expression
Others
CD44+/CD24-
G
SKBR3-dCas9-VP64-MPH
MDA-MB-231-dCas9-VP64-MPH
AC-sgNC
AC-sgNC + Dox
AC-sg1
AC-sg1 + Dox
AC-sg2
AC-sg2 + Dox
Dox (50ng/mL)
OD450
Days
H
AC-sgNC AC-sg1 AC-sg2
SKBR3 -dCas9-VP64-MPH
MDA-MB-231 -dCas9-VP64-MPH
- Dox
+ Dox
I
SKBR3-dCas9-VP64-MPH
AC-sgNC AC-sg1 AC-sg2
- Dox
+ Dox
J
SKBR3-dCas9-VP64-MPH
MDA-MB-231-dCas9-VP64-MPH
AC-sgNC AC-sg1 AC-sg2
-Dox
+Dox
K
KB-sgNC KB-sg2 KB-sg3
L
KB-sgNC KB-sg2 KB-sg3
M
KB-sgNC KB-sg2 KB-sg3

Fig. S4. The effects of *NTN4* overexpression and silencing on breast cancer cells' biological behaviors. Related to Fig. 4.

(A) Pan-cancer expression of *NTN4* in different tumor tissues and corresponding normal tissues analyzed by UALCAN. Boxes represent the median and interquartile range; whiskers extend to the minimum value and maximum value. **(B)**
Boxplot showing relative expression of *NTN4* in normal breast tissues (Normal), luminal breast cancer (Luminal), HER2-positive breast cancer (HER2), and triple-negative breast cancer (TNBC) tissues in the UALCAN database. Each box represents the median and interquartile range. **(C)** Kaplan Meier plotter reveals that *NTN4* expression is positively correlated with the overall survival (OS), the distant metastasis-free survival (DMFS), post-progression survival (PPS) and relapse-free survival (RFS) of breast cancer patients, which is based on *NTN4* mRNA level from the database of the online platform KMplot. Auto select best cutoff was chosen in the analysis. HR, hazard ratio. **(D and E)** qRT-PCR (D) and western blotting (E) detected *NTN4* expression in a panel of benign human breast epithelial cell line (MCF10A) and breast cancer cell lines (other cell lines). **(F)** The expression of *NTN4* is downregulated in human breast cancer stem cells ($CD24^{-}CD44^{+}$) based on expression data GSE7513. **(G)** Cellular proliferation was analyzed by CCK8 in *NTN4* inducible overexpression cell lines SKBR3-dCas9-VP64-MPH with 50 ng/mL Dox. **(H-J)** Representative images of the cellular migration (H), invasion (I) and sphere formation (J) in the indicated *NTN4* inducible overexpression cell lines SKBR3-dCas9-VP64-MPH and MDA-MB-231-dCas9-VP64-MPH as described in Fig. 5c. Scale bar, 50 μm. **(K-M)** Representative images of the cellular migration (K), invasion (L) and sphere formation (M) analyses in *NTN4* knockdown SUM159-dCas9-KRAB cell line as described in Fig. 5h. Scale bar, 50 μm. Data are represented as mean ± SEM. $*P \leq 0.05$, $**P \leq 0.01$, $***P \leq 0.001$. *P* values in figure (A, B, F and G) were calculated using Student's t-test. *P* values in figure (C) were calculated using logrank test. BLCA, Bladder urothelial carcinoma. BRCA, Breast invasive carcinoma. CESC, Cervical squamous cell carcinoma and endocervical adenocarcinoma. CHOL, Cholangio carcinoma. COAD, Colon adenocarcinoma. ESCA, Esophageal carcinoma. GBM, Glioblastoma multiforme. HNSC, Head and Neck squamous cell carcinoma. KICH, Kidney chromophobe. KIRC, Kidney renal clear cell carcinoma. KIRP, Kidney renal papillary cell carcinoma. LIHC, Liver hepatocellular carcinoma. LUAD, Lung adenocarcinoma. LUSC, Lung squamous cell carcinoma. PAAD, Pancreatic adenocarcinoma. PRAD, Prostate adenocarcinoma. PCPG, Pheochromocytoma and paraganglioma. READ, Rectum adenocarcinoma. SARC, Sarcoma. SKCM, Skin cutaneous melanoma. THCA, Thyroid carcinoma. THYM, Thymoma. STAD, Stomach adenocarcinoma. UCEC, Uterine corpus endometrial carcinoma.

Fig. S5.

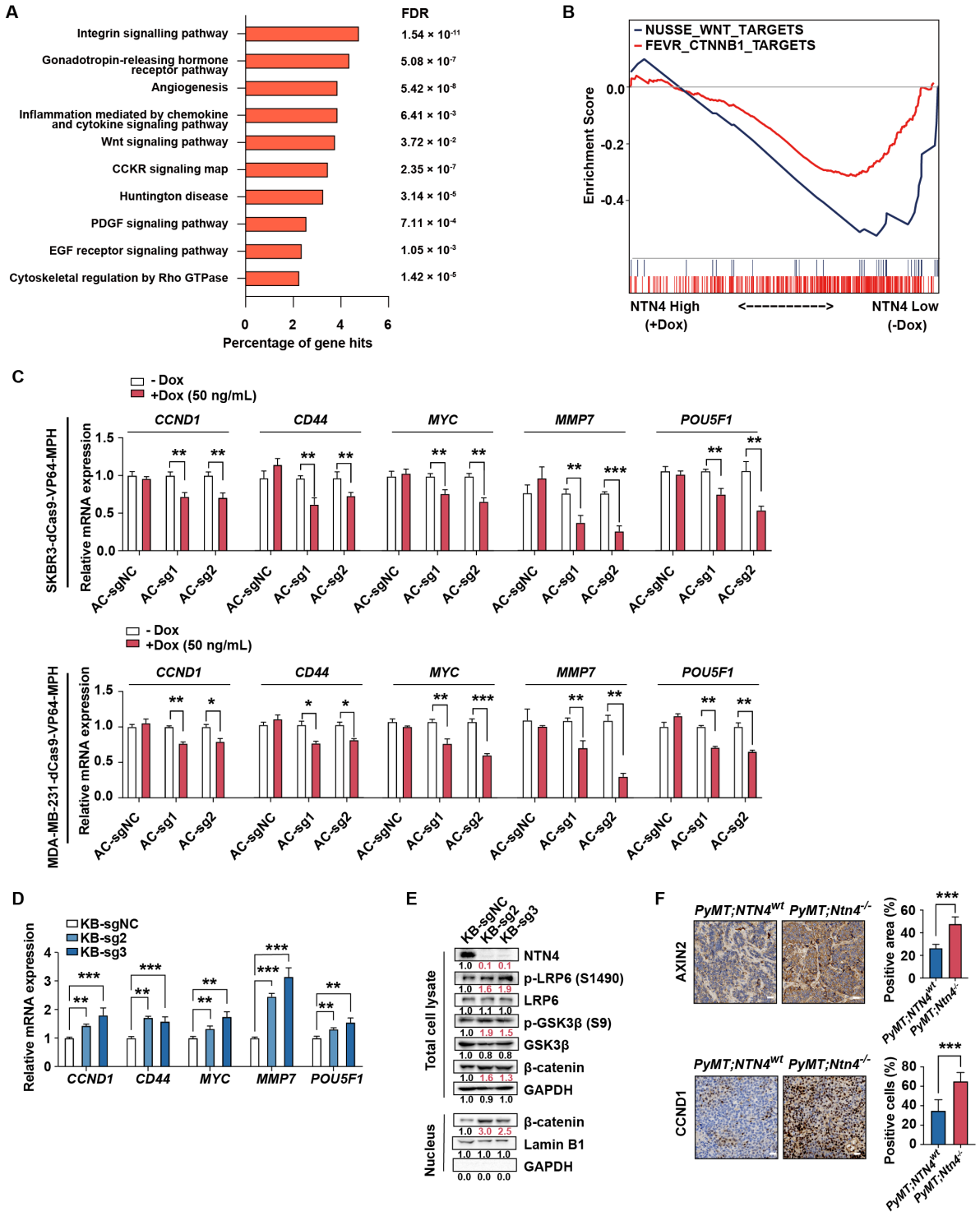

Fig. S5. *NTN4* inhibits the expressions of Wnt/β-catenin signaling target genes. Related to Fig. 5.

(A) Top ten results of PANTHER analysis showing frequencies of differential expression genes from RNA-seq result to pathways indicated. **(B)** GSEA analysis of RNA-seq data for two WNT

target gene signatures, which were NUSSE_WNT_TARGETS (Blue curve: NES = -1.71, FDR q-val = 0.003) and FEVR_CTNNB1_TARGETS (Red curve: NES = -1.45, FDR q-val = 0.027). **(C and D)** qRT-PCR analysis of the Wnt/β-catenin target genes *CCND1, CD44, MYC, MMP7* and *POU5F1* in the *NTN4*-inducible overexpression cell lines SKBR3-dCas9-VP64-MPH and MDA-MB-231-dCas9-VP64-MPH (A) and in the *NTN4* knockdown cells line SUM-159-dCas9-KRAB (B). **(E)** Western blotting analysis of protein levels of p-LRP6, LRP6, p-GSK3β, GSK3β and β-catenin in total cell lysates and nuclear fractions prepared from *NTN4*-knockdown cells SUM-159-dCas9-KRAB. **(F)** Representative images of IHC staining (left) and quantification (right) of AXIN2 and CCND1 in *PyMT;Ntn4*^{wt} and *PyMT;Ntn4*$^{-/-}$ mammary tumors. n = 3 in both groups. Scale bar, 20 μm. Data are represented as mean ± SEM. **P* ≤ 0.05, ***P* ≤ 0.01, ****P* ≤ 0.001. *P* values in figures (C, D and F) were calculated using Student's t-test. Data in figures (C and D) are representative of three independent experiments.

Fig. S6.

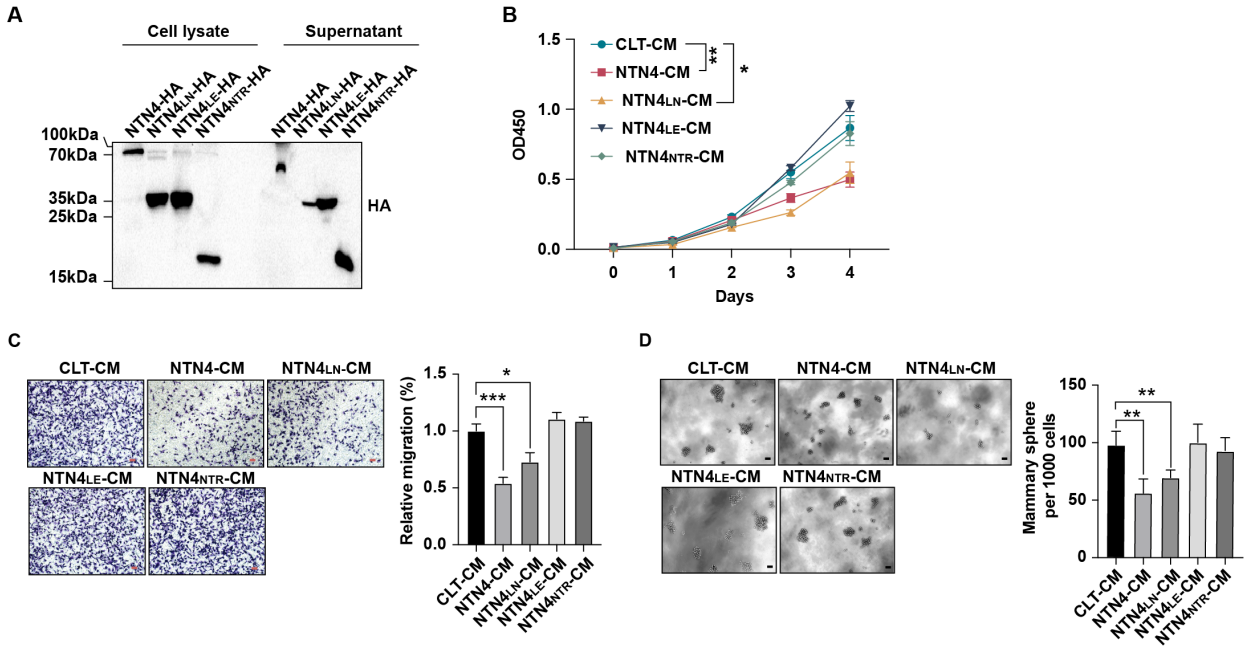

Fig. S6. *NTN4* inhibits breast cancer cell proliferation and metastasis by antagonizing Wnt/β-catenin signaling through its $NTN4_{LA}$ domain. Related to Fig. 6.

(A) Western blot detection of HA-tagged full-length or truncated NTN4 protein in cell lysates and supernatants of 293T cells, which were transiently transfected with full-length or truncated *NTN4* constructs. **(B-D)** Cellular proliferation (B), migration (C) and cancer stem cell features (D) were analyzed in the MDA-MB-231 cell line treated with different condition mediums (CM). Scale bar, 50 μm. Data are represented as mean ± SEM. *p ≤ 0.05, **p ≤ 0.01, ***p ≤ 0.001. *P* values in figures (B-D) were calculated using the Student's t-test. Data are representative of three to six independent experiments.

Supplementary Tables:

Table S1. Summary of LD-SNPs.

Table S2. Gene Expression Omnibus (GEO) identifiers for ChIP-seq, DHSs and ATAC-seq datasets.

Table S3. Summary of LD SNP with enhancer modification in BCAC, GTEX and RegulomeDB database.

Table S4. Characteristics of the breast cancer patients and cancer-free control.

Table S5. Genotypes and allele frequencies of the SNP in enhancer and their associations with the risk of breast cancer.

Table S6. Association of haplotypes and diplotypes of SNPs in enhancer with breast cancer risk.

Table S7. Primer sequences.

Table S8. List of reagents and antibodies.

Table S9. WNT target gene sets used for GSEA.